International Journal of Modern Physics A
Vol. 20, No. 16 (30 June 2005) 3621–3623

World Scientific
www.worldscientific.com

Radiative Penguin Decays of B Mesons: Measurements of $B \to K^*\gamma$, $B \to K_2^*(1430)\gamma$, and Search for $B^0 \to \phi\gamma$

Johannes M. Bauer*

Department of Physics and Astronomy, University of Mississippi–Oxford
University, Mississippi 38677, United States of America
representing the BABAR Collaboration

Electromagnetic radiative penguin decays of the B meson were studied with the *BABAR* detector at SLAC's PEP-II asymmetric-energy B Factory. Branching fractions and isospin asymmetry of the decay $B \to K^*\gamma$, branching fractions of $B \to K_2^*(1430)\gamma$, and a search for $B^0 \to \phi\gamma$ are presented. The decay rates may be enhanced by contributions from non-standard model processes.

Keywords: Radiative Penguin; rare decay; B meson; $K^*\gamma$; $K^*(1430)\gamma$; $\phi\gamma$.

1. Motivation and Data Analysis

The decay of B mesons into $K^*\gamma$ or $K_2^*(1430)\gamma$ is forbidden at the tree-level, but allowed via one-loop $b \to s\gamma$ electromagnetic penguins.[1] Non-standard-model virtual particles may take part in the loop and may affect the decay rate. Non-perturbative hadronic effects make theoretical predictions difficult, but theoretical (as well as experimental) uncertainties are reduced in ratios like the isospin asymmetry Δ_{0-}, expected to be 6 to 13% in the Standard Model (SM):[2]

$$\Delta_{0-} = \frac{\Gamma(\overline{B}^0 \to \overline{K}^{*0}\gamma) - \Gamma(B^- \to K^{*-}\gamma)}{\Gamma(\overline{B}^0 \to \overline{K}^{*0}\gamma) + \Gamma(B^- \to K^{*-}\gamma)}. \quad (1)$$

Penguin annihilation dominates the very clean decay $B^0 \to \phi\gamma$. The branching fraction is only $\mathcal{B}(B^0 \to \phi\gamma) = 3.6 \times 10^{-12}$ in the SM, but higher with R-parity violating supersymmetry.[3]

The results in this report originate from three independent analyses of data collected by the *BABAR* Detector[4] at the asymmetric B Factory, Stanford Linear Accelerator Center (SLAC). The $K^*\gamma$ and the $K_2^*(1430)\gamma$ analyses[5,6] use $(88 - 89) \times 10^6$ $B\overline{B}$ events ($82\,\text{fb}^{-1}$), while the $\phi\gamma$ analysis uses 124×10^6 $B\overline{B}$ events ($113\,\text{fb}^{-1}$).

The hard photon selections are designed to especially remove daughters of π^0 or η. All kaons have to fulfill strict particle identification criteria, and all K^*, $K_2^*(1430)$ or ϕ must satisfy additional requirements, *e.g.*, on their mass.

*Address: SLAC, MS 61, P.O. Box 20450, Stanford, CA 94309, U.S.A.; bauerj@slac.stanford.edu

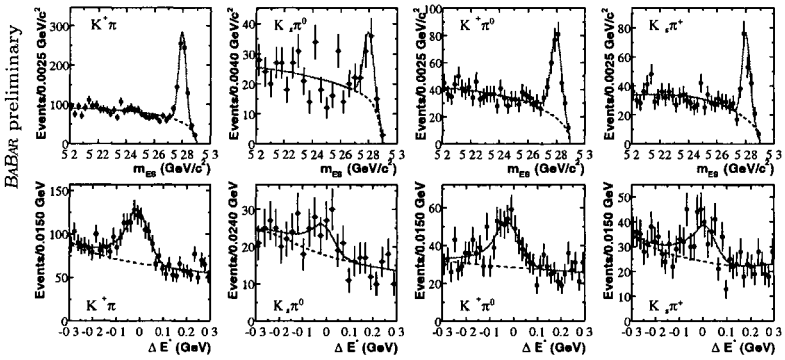

Fig. 1. Distributions of $m_{\rm ES}$ (top) and ΔE^* (bottom) for the four modes in $K^*\gamma$. Besides the data points, the full fit and the background components are shown.

The major background comes from $e^+e^-\to q\bar{q}$ decays (q=u,d,s,c). Their jet-like structure is exploited to distinguish them from the more spherically symmetric $B\overline{B}$ events. For this, all three analyses use neural networks with, *e.g.*, variables based on the directions or flavor of the particles in the event, as well as helicity angles, which make use of correlations between the direction of particles and their daughters.

The final B candidates are described by two variables, $m_{\rm ES} = \sqrt{E^{*2}_{\rm beam} - p^{*2}_B}$ and $\Delta E^* = E^*_B - E^*_{\rm beam}$, with $E^*_{\rm beam}$ the center-of-mass (CM) energy of the e^+/e^- beam, and E^*_B and p^{*2}_B the CM energy and momentum of the B candidate.

2. Analysis of $B \to K^*\gamma$ and $B \to K^*_2(1430)\gamma$

The following modes are reconstructed: $B^0\to K^{*0}\gamma$ with $K^{*0}\to K^+\pi^-$ or $K^0_S\pi^0$, $B^+\to K^{*+}\gamma$ with $K^{*+}\to K^+\pi^0$ or $K^0_S\pi^+$, $B^0\to K^*_2(1430)^0\gamma$ with $K^*_2(1430)^0\to K^+\pi^-$, $B^+\to K^*_2(1430)^+\gamma$ with $K^*_2(1430)^+\to K^+\pi^0$ or $K^0_S\pi^+$.

The number of signal events is extracted via maximum likelihood (ML) fits. The signal shapes in $m_{\rm ES}$ and ΔE^* are described by Gaussian and Crystal Ball functions,[7] while the shapes of $q\bar{q}$ are described by ARGUS functions[8] in $m_{\rm ES}$ and first-order polynomials in ΔE^*. The $B\overline{B}$ background shapes are determined from generic and exclusive Monte Carlo modes. The largest contributor are other $B\to X_s\gamma$ events. For $K^*_2(1430)$, additional events come from $K^*(1410)\gamma$ and non-resonant $B\to K\pi\gamma$ decays, which differ from signal in the $K^*_2(1430)$ helicity angle θ_H.

The ML fits make use of $m_{\rm ES}$ and ΔE^* (Fig. 1), and for $K^*_2(1430)\gamma$ also of the $K^*_2(1430)$ helicity angle (Fig. 2), and lead to the branching fractions listed in Table 1. The isospin asymmetry Δ_{0-}(prelim.) $= 0.050 \pm 0.045$ (stat.) ± 0.028 (syst.) $\pm$ 0.024 ($R^{+/0}$, Ref. 9) is consistent with both the SM and previous measurements.

Table 1. Preliminary branching fractions (1st error statistical, 2nd systematic).

mode	$B^0\to K^{*0}\gamma$	$B^+\to K^{*+}\gamma$	$B^0\to K^{*0}_2(1430)\gamma$	$B^+\to K^{*+}_2(1430)\gamma$
$\mathcal{B}$ ($\times 10^{-5}$)	$3.92 \pm 0.20 \pm 0.24$	$3.87 \pm 0.28 \pm 0.26$	$1.22 \pm 0.25 \pm 0.10$	$1.45 \pm 0.40 \pm 0.15$

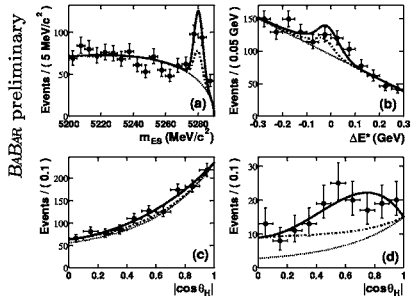

Fig. 2. ML fit for $B^0 \to K_2^*(1430)^0\gamma$ and $K_2^*(1430)^0 \to K^+\pi^-$, with $m_{\rm ES}$ (a), ΔE^* (b), $\cos\theta_H$ (c), and $\cos\theta_H$ in the signal area (d). The points show data, the lines indicate peaking, non-peaking, and signal contributions.

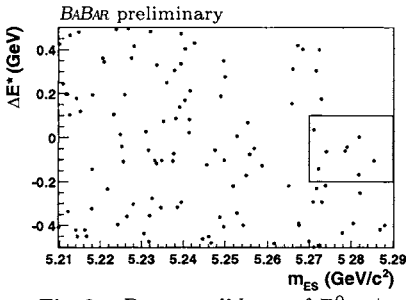

Fig. 3. Data candidates of $B^0 \to \phi\gamma$ in $m_{\rm ES}$-ΔE^* plane. The rectangle at the right side shows the limits of the signal box.

3. Analysis of $\phi\gamma$

The mode $B^0 \to \phi\gamma$ is reconstructed with $\phi \to K^+K^-$. The signal box is defined by $5.27 < m_{\rm ES} < 5.29\,{\rm GeV}/c^2$ and $-0.2 < \Delta E^* < 0.1\,{\rm GeV}$. $B\overline{B}$ background in the signal box is negligible (0.09 ± 0.05 events from Monte Carlo). Continuum background is estimated to be 6 ± 1 events by fitting data events in the $m_{\rm ES}$ and ΔE^* regions outside the signal box and extrapolating into the signal box. Since only eight events were found inside the signal box (Fig. 3), the upper limit[10] for the branching fraction of $B^0 \to \phi\gamma$ is 9.4×10^{-7} at 90% confidence level.

4. Summary and Acknowledgment

All results of this report are preliminary. The branching fractions of $B \to K^*\gamma$ and $B \to K_2^*(1430)\gamma$, as well as Δ_{0-} were measured and are in agreement with previous measurements and SM predictions. The upper limit on the branching fraction of $B^0 \to \phi\gamma$ is currently the tightest published limit on this mode. The lack of signal is consistent with the Standard Model. — The author thanks the *BABAR* collaboration, the SLAC accelerator group and all contributing computing organizations. He was supported by U.S. Dept. of Energy grant DE-FG05-91ER40622.

References

1. K. Lingel, T. Skwarnicki, and J. G. Smith, *Annu. Rev. Nucl. Part. Sci.* **48**, 253 (1998).
2. A. L. Kagan and M. Neubert, *Phys. Lett.* **B539**, 227 (2002); H.-Y. Cheng, C.-K. Chua, *Phys. Rev.* **D69**, 094007 (2004).
3. Y. D. Yang, *Eur. Phys. J.* **C36**, 97 (2004).
4. B. Aubert *et al.* (*BABAR* Collaboration), *Nucl. Instr. and Methods* **A479**, 1 (2002).
5. B. Aubert *et al.* (*BABAR* Collaboration), hep-ex/0407003 (2004), submitted to PRL.
6. B. Aubert *et al.* (*BABAR* Collaboration), hep-ex/0409035 (2004), submitted to PRD.
7. E. D. Bloom and C. W. Peck, *Annu. Rev. Nucl. Part. Sci.* **33**, 143 (1983).
8. H. Albrecht *et al.* (ARGUS Collaboration), *Z. Phys.* **C48**, 543 (1990).
9. B. Aubert *et al.* (*BABAR* Collaboration), *Phys. Rev.* **D69**, 071101 (2004).
10. R. D. Cousins and V. L. Highland, *Nucl. Instr. and Methods* **A320**, 331 (1992); G. J. Feldman and R. D. Cousins, *Phys. Rev.* **D57**,3873 (1998).